TISSUE ENGINEERING: Part A
Volume 21, Numbers 9 and 10, 2015

DOI: 10.1089/ten.tea.2014.0474

Heparin Binding–Epidermal Growth Factor-Like Growth Factor for the Regeneration of Chronic Tympanic Membrane Perforations in Mice

Peter Luke Santa Maria, MBBS, PhD,[1] Sungwoo Kim, PhD,[2]
Yasin Kursad Varsak, MD,[1] and Yunzhi Peter Yang, PhD[2,3]

We aim to explore the role of epidermal growth factor (EGF) ligand shedding in tympanic membrane wound healing and to investigate the translation of its modulation in tissue engineering of chronic tympanic membrane perforations. Chronic suppurative otitis media (CSOM) is an infected chronic tympanic membrane perforation. Up to 200 million suffer from its associated hearing loss and it is the most common cause of pediatric hearing loss in developing countries. There is a need for nonsurgical treatment due to a worldwide lack of resources. In this study, we show that EGF ligand shedding is essential for tympanic membrane healing as it's inhibition, with KB-R7785, leads to chronic perforation in 87.9% ($n = 58$) compared with 0% ($n = 20$) of controls. We then show that heparin binding–EGF-like growth factor (5 μg/mL), which acts to shed EGF ligands, can regenerate chronic perforations in mouse models with 92% (22 of 24) compared with 38% (10 of 26), also with eustachian tube occlusion with 94% (18 of 19) compared with 9% (2 of 23) and with CSOM 100% (16 of 16) compared with 41% (7 of 17). We also show the nonototoxicity of this treatment and its hydrogel delivery vehicle. This provides preliminary data for a clinical trial where it could be delivered by nonspecialist trained healthcare workers and fulfill the clinical need for a nonsurgical treatment for chronic tympanic membrane perforation and CSOM.

Introduction

According to the World Health Organization (WHO), an estimated 39–200 million individuals suffer from chronic suppurative otitis media (CSOM) associated hearing loss and it is the most common cause of persistent hearing impairment among children in the developing countries.[1] The current standard of care is surgery to restore integrity of the tympanic membrane (TM), improve hearing, and reduce further incidence of infection.[2] However, initial graft take rates can be as low as 65%.[2,3] Third world countries lack the surgical resources to address the demand and so many go untreated.[4] Because of this great unmet clinical need, a nonsurgical treatment for chronic TM perforation has been identified as potentially the greatest advance in otology since the cochlear implant.[5] Many nonsurgical attempts for treating chronic TM perforations have been investigated, but are yet to demonstrate superiority to surgery.[6] In an ideal setting, a therapeutic, bioresorbable implant would readily be administered locally and deliver the effective bioagents to accelerate or enable the healing of chronic TM perforations.

In recognition of their potential impact for treatment, bioactive substances have long been pursued in TM wound healing with attempts to either inhibit or promote healing.[7,8] These include fibroblast growth factor 1[9] and 2,[10–13] various subtypes of platelet-derived growth factor,[14,15] hyaluronic acid,[16–18] and epidermal growth factor (EGF).[19,20] Until now these attempts have had poor efficacy or require adjunctive surgical procedures to be performed, such as microscopic excision of the perforation margin. If a bioactive substance requires specialist training, general anesthesia or microscopic-assisted surgery then it does not address the clinical need.

To address the worldwide clinical need, we aimed to develop a novel, clinically applicable, therapeutic, bioresorbable implant with heparin binding epidermal growth factor-like growth factor, also known as heparin binding–epidermal growth factor (HB-EGF), to treat chronic TM perforations in the presence of bacteria or Eustachian tube (ET) dysfunction. By doing so, we explore for the first time, the effect of HB-EGF as a therapeutic on wound healing in the TM. The accomplishment of this project establishes the foundation for future research toward developing first in human studies of HB-EGF treatment of chronic TM perforations.

Departments of [1]Otolaryngology, Head and Neck Surgery, [2]Orthopedic Surgery, and [3]Materials Science and Engineering, Stanford University, Stanford, California.

Materials and Methods

All animal work was approved by Stanford's Administrative Panel on Laboratory Animal Care.

All mice used for all experiments were 6–10 week old male CBA/CAJ (15–25 g) mice purchased from Jackson Laboratories. All otoscopy and surgical interventions were performed using inhaled isoflurane at 3–4% for induction and 1–2% for maintenance. For the ET occlusion surgery to create mouse models 2 and 3 described below, twice daily intramuscular buprenorphine (0.01–0.05 mg/kg) was given for 48 h postoperatively. Determination of animal numbers was performed using the STATA version 13 aiming for an α of 0.05, a β of 0.8. We also made provisions for potential animal mortality and failure to establish a chronic perforation.

Polymer construction

The polymer construction was performed according to a previously published technique and its release of added growth factors have been characterized.[21–23] The mass ratio of chitosan to lactide was 8:1. 3.3 mM. Sodium metabisulfite was added into the prepolymer solution to form a cross-linked hydrogel within a few minutes.

Creating mouse models of chronic TM perforation

Three animal models of chronic TM perforation were developed and are described below. Each successive model attempts to better mimic the human condition. The first model is a model of dry chronic TM perforation. The second model is a model of chronic TM perforation with ET occlusion. The third model is a model of CSOM. When the endpoints in the models were achieved, all animals were sacrificed with half of the tissue used for histology and the other half processed for immunohistochemistry.

Mouse model of chronic TM perforation (model 1)

A previously published technique to create TM perforations in rats was adapted to mice. A curved micro needle is used to create a subtotal perforation in the pars tensa of the TM.[24] The mice TMs either had 10 mM KB-R7785 (4-(N-hydroxyamino)-2R-isobutyl-3S-methylsuccinyl)-L-phenylglycine-N-methylamide, also known as OSU8-1) ($n=70$) or 0.9% normal saline ($n=20$) injected onto gel foam (the gel foam was placed through and onto the perforation at the time of creating the perforation) over 7 days following perforation. Both TMs of the mice, either both allocated to KB-R7785 or saline groups, were used. KB-R7785 for all animal experiments was obtained as a gift from Dr Higashiyama's lab in Ehime University, Japan. Two mice in the KB-R7785 group were sacrificed at various time points (day 2, 7, 14, 30, 44, 60) and had tissue processed for histology to observe the effects on keratinocyte migration, leaving a total of 58 mice TMs to evaluate for the presence of chronic perforation at 3 months. The endpoint for a chronic perforation is one that has remained open for a period of 3 months.

Mouse model with surgery for ET obstruction (model 2)

The procedure in the rat[25] was adapted by opening the bulla using an engraving device with a 0.5 mm burr. In brief, a hole is be drilled (engraving device with a 0.5 mm burr) at the midpoint along the length of the bony ET, the membranous cover will be opened, and small pieces of Gutta Percha Points (Meta Biomed) placed into the defect and melted using electrocautery to conform to the lumen. The mice were allowed to recover from this procedure for 4 weeks before creating chronic TM perforations (as described in model 1). The mice were then treated with either HB-EGF or control as described below. A total of 42 mice with unilateral chronic TM perforations and ET occlusion comprised this group.

Mouse model of CSOM (model 3)

To create a mouse model for CSOM, the above chronic perforation model with ET obstruction was first created unilaterally. The perforation was then untouched for 3 months. Otoscopy, under general anesthesia, was performed to verify persistence of the perforation. The bacteria chosen were two of the most commonly involved in chronic ear disease, *Streptococcus pneumoniae* type 3 (ATCC strain 6303 dose of 6×10^6 colony forming units per mL) and *Pseudomonas aeruginosa* (ATCC strain CRM27853 dose of 6×10^9 colony forming units per mL). These bacteria were purchased directly from ATCC and were prepared according to their accompanying protocols. *Streptococcus pneumoniae* type 3 was prepared in ATCC broth #44 and plated in #260 agar. *Pseudomonas aeruginosa* was prepared in ATCC #18 broth and plated in #18 agar. After creating the chronic perforation model with ET occlusion, one of the two types of bacteria were inoculated into the middle ear through the existing chronic perforations. The bacteria were delivered into the middle ear through the created perforation through the external auditory canal.

The pseudomonas group formed CSOM group 1 ($n=16$), that is, 16 mice with unilateral pseudomonas CSOM. The streptococcus group formed CSOM group 2 ($n=17$), that is, another 17 mice with pseudomonas CSOM. At 2 weeks the ear fluid from one mouse from each cage (mice kept in groups of four or five) was collected through micro swab and sent for polymerase chain reaction (PCR), performed by the Department of Comparative Medicine at Stanford, to test for the presence of bacteria. All the sampled mice ($n=4$) from CSOM group 1 were *Pseudomonas aeruginosa* PCR positive at 2 weeks. All the sampled mice ($n=4$) in CSOM group 2 were streptococcus PCR negative at 2 weeks. The mice in CSOM group 2 then had pseudomonas inoculated as for the first group. PCR was then performed from one mouse from each cage in CSOM group 2 ($n=4$) and all were positive for pseudomonas at 2 weeks. This gave two cohorts of CSOM mice. CSOM 1 had pseudomonas only, whereas CSOM 2 had failed chronic inoculation of streptococcus before having successful chronic inoculation of pseudomonas. The mice were then treated with either HB-EGF or control as described below. All mice from CSOM groups 1 and 2 were caged only with other mice within the same CSOM group. This prevented cross contamination of bacteria between mice of different groups.

HB-EGF treatment

In all treatment groups, recombinant mouse proheparin-binding EGF-like growth factor (proHB-EGF) purchased from Prospec (catalogue number CYT-068) was used at 5 μg/mL delivered by the above-described hydrogel polymer. The treatment was injected through the external auditory canal,

using a syringe and 27-gauge needle, through and onto the TM to fill the middle ear and into the external ear. The total volume delivered was ~0.4 mL in each case. In control ears, only the hydrogel polymer was injected. TMs were evaluated at 4 weeks, when the hydrogel was no longer visible in the ear canal.

After creating animal model 1 (chronic perforation model), chronic TM perforations were either injected with HB-EGF treatment ($n=24$) or a control with the hydrogel only ($n=26$). TMs were evaluated at 4 weeks, when the hydrogel was no longer visible in the ear canal. As the mice in this group contained bilateral chronic TM perforations, each mouse received the same treatment in both ears to minimize the risk of cross contamination with treatment.

After creating animal model 2 (chronic perforation with ET occlusion model), chronic perforations were either injected with HB-EGF treatment ($n=19$) or a control with the hydrogel only ($n=23$). TMs were evaluated at 4 weeks, but the hydrogel was still visible over the TM in most case and, therefore, the TMs were reevaluated at 6 weeks, when the hydrogel was no longer visible in the ear canal.

After creating animal model 3 (CSOM model), chronic perforations were either injected with HB-EGF treatment ($n=16$) or a control with the hydrogel only ($n=17$). This contained a cohort created of pseudomonas only with treatment ears ($n=8$) and control ($n=8$) and a cohort with pseudomonas following failed chronic streptococcus inoculation with treatment ears ($n=8$) and control ($n=9$). TMs were evaluated at 4 weeks, when the hydrogel was no longer visible in the ear canal.

Otoscopy

Otoscopy was performed under general anesthesia using a Welch Allyn Digital MacroView Otoscope.

Histology

Histology was performed using Hematoxylin and Eosin staining according to a previously published technique.[24]

Immunohistochemistry

To observe the keratin and keratinocyte layers of the TMs. Cytokeratin staining was performed using Monoclonal Mouse Anti-Human Cytokeratin Clone MNF116 (Cat #M 0821; Dako) and a previously published technique.[26]

Polymer ototoxicity assay

The polymer was injected through an acute TM perforation in 12 mice. Hearing was measured at intervals in 3 mice (auditory brainstem response [ABR] and distortion product otoacoustic emission [DPOAE]) and compared with the control side, which had the polymer injected only to understand how long the polymer may remain in the middle ear. The rest of the cohort was then measured at day 60, a time after which it was thought the hearing was likely to have returned to baseline.

HB-EGF ototoxicity assay

HB-EGF was injected at a dose 10 times (50 μg/mL) the effective dose (5 μg/mL) with the polymer through an acute TM perforation in 13 mice. This dose was chosen according to guidelines provided by regulatory FDA consultation. Hearing was measured at 10 weeks (ABR and DPOAE) and compared with the control side, which had the polymer injected only.

Photographic recording

All transcanal photographs were taken with a Digital MacroView Otoscope (Welch Allyn).

Hearing threshold measurements

ABR and DPOAE measurements were taken as previously described.[27] Frequencies measured were 4.0, 5.7, 8.0, 11.3, 16.0, 23.0, 31.9, and 46.1 kHz. When the pure tone average was calculated, the mean of all the above-listed frequencies was used. Briefly, the ABR potentials were measured through needle electrodes positioned in the postauricular tissue and at the vertex of the head, with a ground electrode placed in the rear leg. A bioamplifier (DP-311; Warner Instruments) amplified the signal 10,000 times. The sound intensity level was raised in 10 dB steps (10 to 80 dB) SPL. At each sound level, 260 responses were measured and averaged. At each frequency, the peak-to-peak value of the ABR was measured and the threshold was calculated as when this value was five standard deviations above the noise floor. The threshold was set arbitrarily at 80 dB SPL for averaging purposes, if an ABR response was not detected at 80 dB SPL. DPOAEs were measured in the external auditory canal by a probe tip microphone (type 4182; Brüel & Kjaer). The frequency response of this microphone was measured using a free-field microphone with a flat frequency response out to 100 kHz (type 4939; Brüel & Kjaer). This calibration curve was then used to adjust the DPOAE amplitudes. The sound stimuli for eliciting DPOAEs were two 1 s sine-wave tones of differing frequencies ($F2=1.22\times F1$). F2 ranged from 4 to 46.1 kHz. The two tones were of equal intensities and stepped from 20 to 80 dB SPL in 10 dB increments. The amplitude of the cubic distortion product was measured at $2\times F1–F2$. The threshold at each frequency was calculated to be when the DPOAE was more than five dB SPL and two standard deviations above the noise floor. The threshold was set arbitrarily at 80 dB SPL for averaging purposes, if an DPOAE was not detected at 80 dB SPL.

Statistical analysis

STATA version 13.0 was used for analysis. For all statistical analysis a two-tailed Student's *t*-test was performed. A significance level of 0.05 was used for the null hypothesis.

Results

The experimental protocol and results are summarized in Table 1.

Inhibition of epidermal growth factor receptor ligand shedding creates a chronic TM perforation (model 1)

Control TM perforations, treated with saline only, all (100%) closed in 2 weeks ($n=20$) compared with 87.9% (51 of 58) of the KB-R7785-treated ears ($p<0.01$) (Supplementary Fig. S1; Supplementary Data are available online at www.liebertpub.com/tea). In the KB-R7785 group, keratinocyte migration was not only inhibited during its use in the

Table 1. Experimental Protocol and Outcomes

Chronic perforation model creation	*TMs (*n*)*	*Outcome (% chronic perforations)*
Mouse model of chronic TM perforation (model 1)—total		
KB-R7785 group	58	87.9% (51 of 58)
Saline group	20	0% (0 of 20)
Mouse model with surgery for eustachian tube obstruction (model 2)		
KB-R7785 group	42	100% (42 of 42)
Mouse model of CSOM (model 3)—CSOM group 1		
KB-R7785 group	16	100% (16 of 16)
Mouse model of CSOM (model 3)—CSOM group 2		
KB-R7785 group	17	100% (17 of 17)
HB-EGF treatment of chronic perforations		*Outcome (% complete closure of perforation)*
Mouse model of chronic TM perforation (model 1)—total	50	
Treatment group	24	92% (22 of 24)
Control group	26	38% (10 of 26)
Mouse model with surgery for eustachian tube obstruction (model 2)	42	
Treatment group	19	94% (18 of 19)
Control group	23	9% (2 of 23)
Mouse model of CSOM (model 3)—CSOM group 1	16	
Treatment group	8	100% (8 of 8)
Control group	8	50% (4 of 8)
Mouse model of CSOM (model 3)—CSOM group 2	17	
Treatment group	8	100% (8 of 8)
Control group	9	33.3% (3 of 9)
Mouse model of CSOM (model 3)—CSOM groups combined	33	
Treatment group	16	100% (16 of 16)
Control group	17	41% (7 of 17)

Table shows the outcomes of the creation of the chronic perforation models as well as the HB-EGF treatment in these models.
CSOM, chronic suppurative otitis media; HB-EGF, heparin binding–epidermal growth factor; TM, tympanic membrane.

first week, but through the following 3 months. The TM wounds fails to exhibit significant keratinocyte proliferation and migration during the 3 months (Fig. 1). On day 2 (Fig. 1a) the perforation margins can be seen with debris over the perforation. There is a lack of inflammatory infiltrate within the debris and the TM is not thickened. On day 7 there is a lack of proliferative activity seen at the handle of the malleus with no new TM forming from the attachment. There is a lack of Cytokeratin staining (Fig. 1b) seen in the residual TM suggesting a lack of proliferation and migration of keratinoctyes. On day 44 (Fig. 1c) the TM is still thin with a nonhealed perforation. The lack of proliferative activity at the handle of the malleus is still evident with a lack of Cytokeratin staining (Fig. 1d) seen. This suggests that keratinocyte migration is essential for normal healing of the TM. It also demonstrates that this process can be inhibited long after the initial period of application of KB-R7785. The TM does not recover to heal within 3 months. This provides the validation for our chronic perforation model 1.

Chronic TM perforations with ET dysfunction (model 2)

One hundred percent ($n=42$) of perforations in mice with KB-R7785 applied following surgery to occlude the ET became chronic. When compared with the above cohort with chronic perforations created without ET occlusion (51 of 58), there was a significant difference with those perforations with ET occlusion more likely to become chronic when applying KB-R7785 ($p=0.04$). The perforations with ET occlusion, in contrast to the chronic perforations without, were wet with mucoid otorrhea. The TMs were more opaque, thickened, and reddened in the areas that did heal (Supplementary Fig. S2). The middle ear mucosa was seen to be thickened and inflamed with the presence of cilia lining the middle ear mucosa and an inflammatory exudate visible within the middle ear cavity (Fig. 2).

The first animal model for CSOM (model 3)

One hundred percent ($n=8$) of specimen sampled mice from our CSOM model were PCR positive at 2 weeks indicating continuing presence of bacteria and validating our model of CSOM. This compares with 0% ($n=4$) of our attempts to create a CSOM model with streptococcus pneumonia type 3. Figure 3 demonstrates the perforation edge in this CSOM model. The perforation edge shows a mucosal layer migrated laterally to be directly adjacent to the keratinocyte layer with a thickened fibrous layer containing inflammatory cells.

HB-EGF heals chronic TM perforations

When a cohort of chronic perforations in mice ears (model 1) were treated with a single dose (40 μL) of HB-EGF

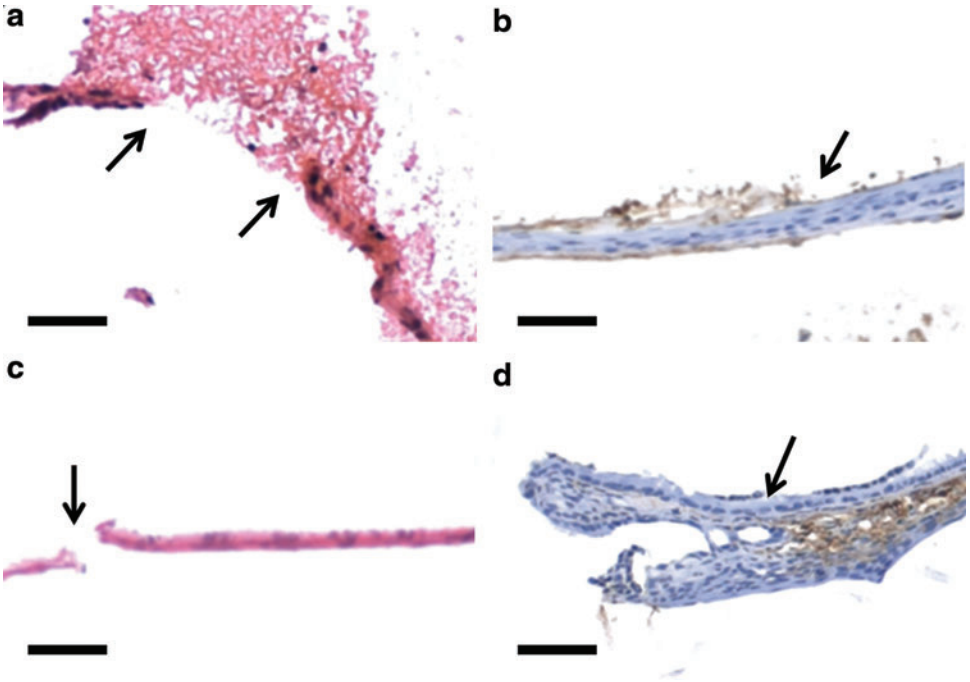

FIG. 1. Developing KB-R7785 chronic tympanic membrane (TM) perforations. Figure demonstrates the lack of progression, through the proliferation and migration of keratinocytes of the TM wound following perforation and application of KB-R7785 with staining with Hematoxylin and Eosin **(a, c)** and Cytokeratin **(b, d)**. Time points are day 2 **(a)**, showing the perforation edge (*arrow*) and surrounding exudate, day 7 **(b)**, showing keratinization inhibited (*arrow*), and day 44 **(c)**, showing a perforation (*arrow*) and no keratinization, day 44 **(d)** showing a lack of keratinocyte proliferation at the handle of malleus attachment to the TM (*arrow*). Scale bar = 10 μm (magnification 10×). Color images available online at www.liebertpub.com/tea

5 μg/mL, 92% (22 of 24) healed, with complete closure of the perforation, compared with 38% (10 of 26) of controls (polymer only), where perforations were still present, at 4 weeks ($p < 0.01$) (Fig. 4). The healed treated TMs (Fig. 4a), from the chronic TM perforation group, have a similar macroscopic appearance to the normal TM.

This demonstrates the efficacy of HB-EGF in this model of chronic perforation. The mechanism is likely to be epidermal growth factor receptor (EGFR) ectodomain ligand shedding mediated keratinocyte migration.[28] Healing of the chronic perforations in the treatment group has the appearance of normal TMs with increased production of keratin. In the cases which healed in the control, there was a lack of a distinct keratinocyte layer and thickening of the fibrous layer (Fig. 5). There were no cases seen in the control ears, without HB-EGF treatment, that showed normal TM wound healing with a normal keratinocyte layer. Without HB-EGF, the TM may still be able to close the perforation in some

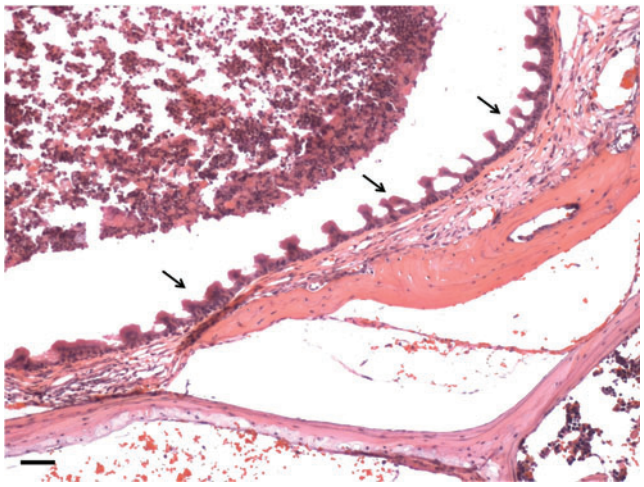

FIG. 2. Changes in the middle ear with eustachian tube (ET) occlusion. Figure demonstrates the changes in the middle ear mucosa with occlusion of the ET. Cilia are present in the mucosa of the middle ear mucosa (*arrows*) with an inflammatory exudate (*top left corner*). These changes are seen throughout the middle ear mucosa in models created with ET occlusion. They are not seen in models without ET occlusion. Scale bar = 10 μm (magnification 10×). Color images available online at www.liebertpub.com/tea

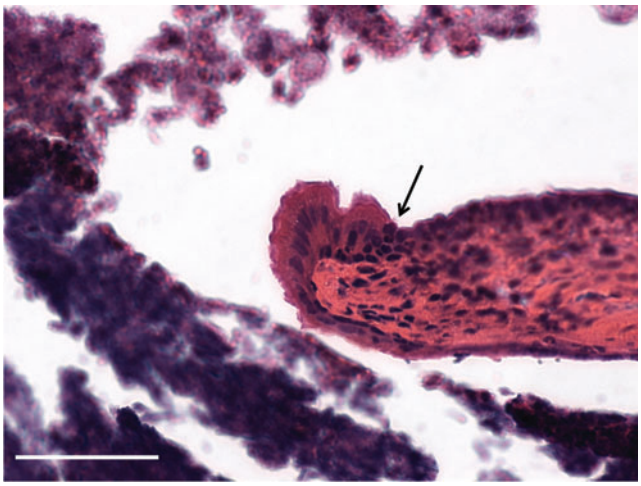

FIG. 3. The perforation margin in the chronic suppurative otitis media (CSOM) model. Figure demonstrates the perforation edge showing a mucosal layer migrated laterally to be directly adjacent to the keratinocyte layer (*arrow*) with a thickened fibrous layer containing inflammatory cells. These findings are commonly observed in human chronic TM perforations. Scale bar = 10 μm (magnification 40×). Color images available online at www.liebertpub.com/tea

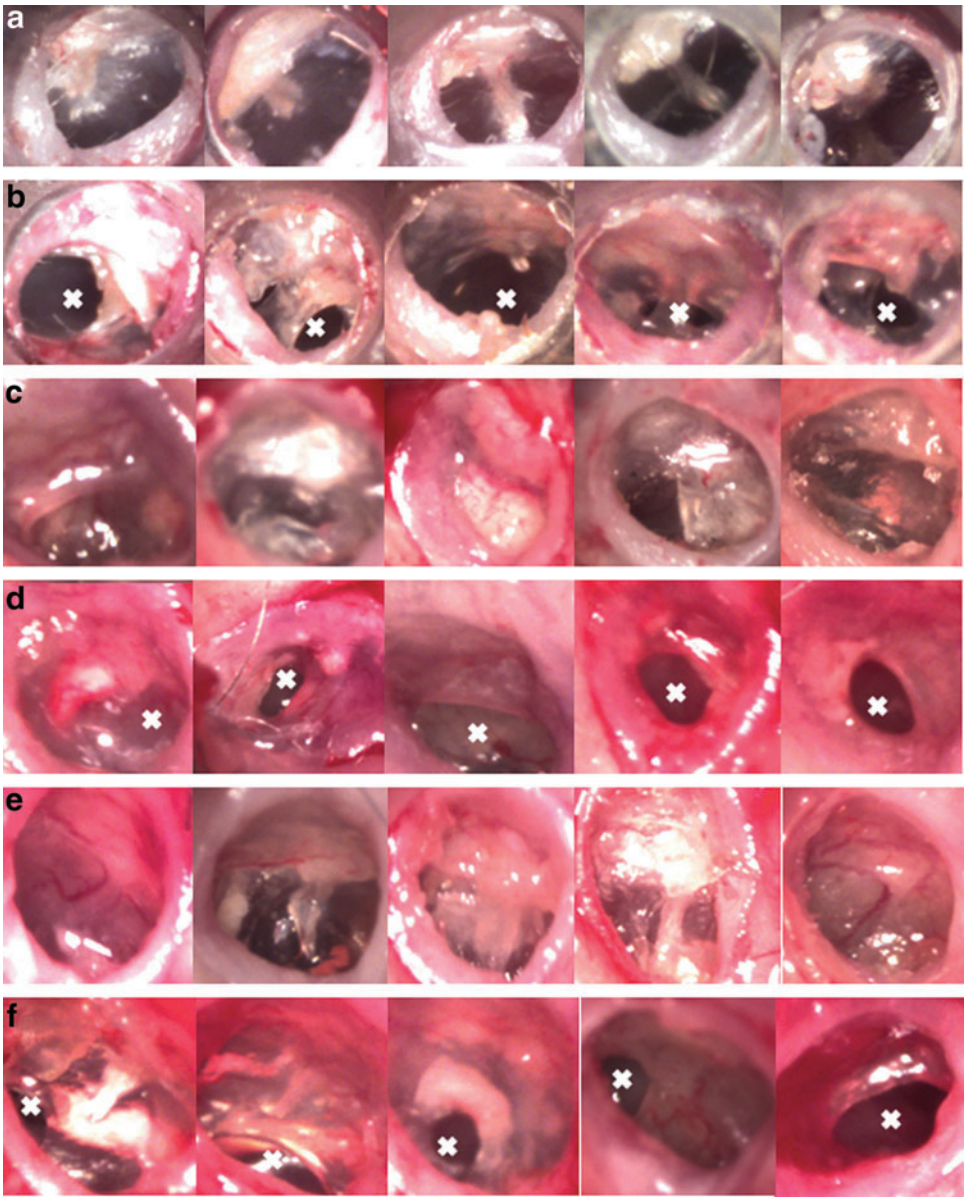

FIG. 4. Heparin binding–epidermal growth factor (HB-EGF) treatment of chronic TM perforations. Figure shows the otoscopic appearance of chronic TMs treated with HB-EGF **(a)** and those controls treated with polymer only **(b)** at 4 weeks following treatment. Figure also shows the otoscopic appearance of chronic TMs with ET occlusion treated with HB-EGF **(c)** and those controls treated with polymer only **(d)** at 6 weeks following treatment. Figure also shows the otoscopic appearance of CSOM treated with HB-EGF **(e)** and those controls treated with polymer only **(f)** at 4 weeks following treatment. A *white X marks* the area of residual perforation. Color images available online at www.liebertpub.com/tea

cases, but they are unable to heal with the normal histological layers of the TM. The keratinocyte layer is required for normal TM function. Without a keratinocyte layer, in the clinical situation, there is a predisposition for the TM to develop granular myringitis.[29]

When a cohort of mice from model 2 (chronic perforations and ET occlusion) of chronic TM perforations were treated with recombinant HB-EGF 5 μg/mL (sustained release dose through a bioabsorbale chitosan–lactide-based polymer), 94% (18 of 19) healed, with closure of the TM

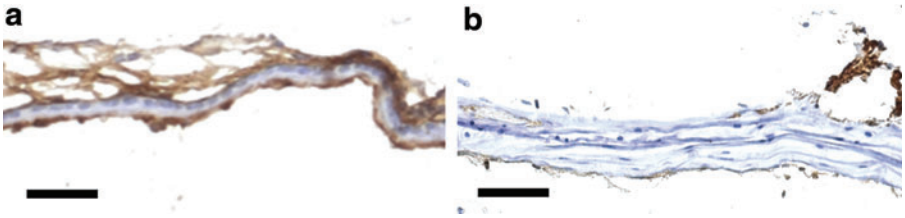

FIG. 5. The healed TM following HB-EGF treatment compared with healed controls. Figure shows Cytokeratin (*brown*) staining to identify the keratinocytes and keratin layers in the TM. The HB-EGF-treated chronic perforation **(a)** shows normal TM layers, including a thick keratin layer compared with the control TM **(b)**. The HB-EGF-treated TM **(a)** has a normal thickness connective tissue layer compared with the lack of keratinization and thick disorganized connective tissue layer of the control TM **(b)**. Scale bar = 10 μm (magnification 40×). Color images available online at www.liebertpub.com/tea

perforation, compared with 9% (2 of 23) of controls (polymer only), with residual perforations, at 6 weeks ($p < 0.01$). Macroscopically, the healed TMs had a normal appearance in some cases, but had thickened opaque TMs with and without retraction of the pars tensa in others (Fig. 4). The healed, treated TMs in the ET occlusion setting (Fig. 4c) demonstrate retraction (first and fifth panels) or opaque thickening (second, third, and fourth panels) in some circumstances. In the control, polymer only group in the ET occlusion setting (Fig. 4d) the perforations were wet with red thickening of the TM. Healing in the presence of ET occlusion showed macroscopic differences to those without ET occlusion. Histologically, the HB-EGF-treated TMs closed and had a similar appearance to the above model, with normal layers of the TM and some areas of increased keratin formation. In comparison, the controls showed a lack of keratinocytes even in those few cases where closure occurred. This demonstrates that HB-EGF was able to successfully heal chronic TM perforations with normal histological layers in the setting of ET occlusion. The middle ear mucosa in both the HB-EGF-treated and control groups often showed the same inflammatory changes described in the ET occlusion chronic TM model at 3 months. There is an increase in cilia seen lining the middle ear mucosa and an inflammatory exudate seen in the middle ear cavity. Despite this inflammatory process continuing through the middle ear, all treated TMs were able to heal.

Treating a cohort of mice with the CSOM model (model 3) created as described above with recombinant HB-EGF 5 μg/mL (sustained release dose through a bioabsorbable chitosan–lactide-based polymer) 100% (16 of 16) healed, with complete perforation closure, compared with 41% (7 of 17) of controls (polymer only), with failure to close the perforation, at 4 weeks ($p < 0.01$). Looking at these cohorts broken down into those who had pseudomonas only and those that had failed streptococcus chronic inoculation, there was no difference between these cohorts. The pseudomonas only cohort had 100% (8 of 8) in the treatment group compared with 50% (4 of 8) in the control group ($p < 0.01$). The pseudomonas after failed streptococcus chronic inoculation group had 100% (8 of 8) in the treatment group compared with 33.3% (3 of 9) in the control group ($p < 0.01$). The difference in healing of the control groups of both CSOM cohorts was not significant ($p = 0.52$).

Macroscopically the healed TMs had a normal appearance in some cases, but had thickened opaque TMs in others (Fig. 4). The healed treated TMs in the CSOM model (Fig. 4e) demonstrate near normal appearance (second panel), middle ear effusion (first, third, fifth panels) and areas of opaque thickening (fourth panel) in some circumstances. In the control, polymer only group in the CSOM model (Fig. 4f) the perforations were wet with red thickening of the TM. In some cases, the gutta percha can still be clearly seen in the middle ear (first and second panels of Fig. 4f). Unlike in the ET occlusion only model, there were no cases of healed TMs with retraction. Histologically, the HB-EGF-treated TMs also showed normal TM layers with some showing increased keratin. As for the other models, the controls showed a lack of keratinocytes and keratin formation. This demonstrates the ability of HB-EGF to successfully heal CSOM with normal histological layers. As for the ET occlusion model, there were also some specimens with an increase in cilia seen lining the middle ear mucosa and an inflammatory exudate seen in the middle ear cavity. There did not seem to be any relation to middle ear mucosal changes and incidence of healing of the TM. This is the first and only growth factor treatment tested in an animal model of CSOM that has shown significant benefit over control.

Biodegradable polymer for HB-EGF delivery

For future use in the human ear, we demonstrated the nonototoxicity of the hydrogel polymer in mice ears following perforations. A conductive hearing loss can be expected when the ear is filled with polymer until the polymer absorbs. At first a sample ($n = 3$) of the polymer-treated ears were tested with ABR thresholds at serial time points until they reached the level of the control ears ($n = 3$) at 60 days. This demonstrated that the polymer was present in the middle ear and causing hearing loss until this time (Supplementary Fig. S3). When the full cohort of mice were tested, there was no difference in ABR and DPOAE thresholds measured at 60 days ($n = 9$ in each group) (Supplementary Fig. S4). Histological specimens did not demonstrate any additional inflammatory reaction or changes when compared with the control.

HB-EGF is not ototoxic in the mouse model

When HB-EGF was injected at 10 times the effective dose (50 mg/mL) with the polymer through an acute TM perforation, there was no difference in hearing when measured at 10 weeks (ABR and DPOAE) (Fig. 6) and at 16 weeks (Supplementary Fig. S5) compared with the control side, which had the polymer injected only. Furthermore, there was no difference between sides in histological inflammatory changes in the middle ear or cochlea.

Discussion

The histology of TM wound healing is well known.[24] Wound healing in the TM is similar to cutaneous wound healing, except that it occurs in midair. The malleus plays a crucial role in the healing of the TM being the site for significant mitotic activity during the healing process. Migration of keratinocytes across layers of the TM appears to account for the closure of the perforation.[24] TM wound healing has not previously been studied in the presence of bacteria or ET dysfunction. This is important as the presence of infection and ET dysfunction is known to clinically affect healing in the middle ear and the TM.[7,30]

When examining the literature in this area, it is also important to make the distinction between acute and chronic wounds. Chronic wounds, by definition, have failed to progress through the usual orderly and timely process of wound healing without establishing a sustained anatomic and functional result.[31] Acute TM perforations will all heal whereas chronic TM perforations have demonstrated an inability to heal over 3 months.[23]

HB-EGF was previously identified to be significant in acute wound healing of the TM.[32] KB-R7785, a hydroxamate-based metalloproteinase inhibitor, is an inhibitor of EGFR ligand shedding reducing expression of HB-EGF, amphiregulin, and tumor necrosis factor-α. HB-EGF inhibition accounts for the large majority of its effects.[26] Based on the hypothesis that HB-EGF-induced EGFR ligand shedding

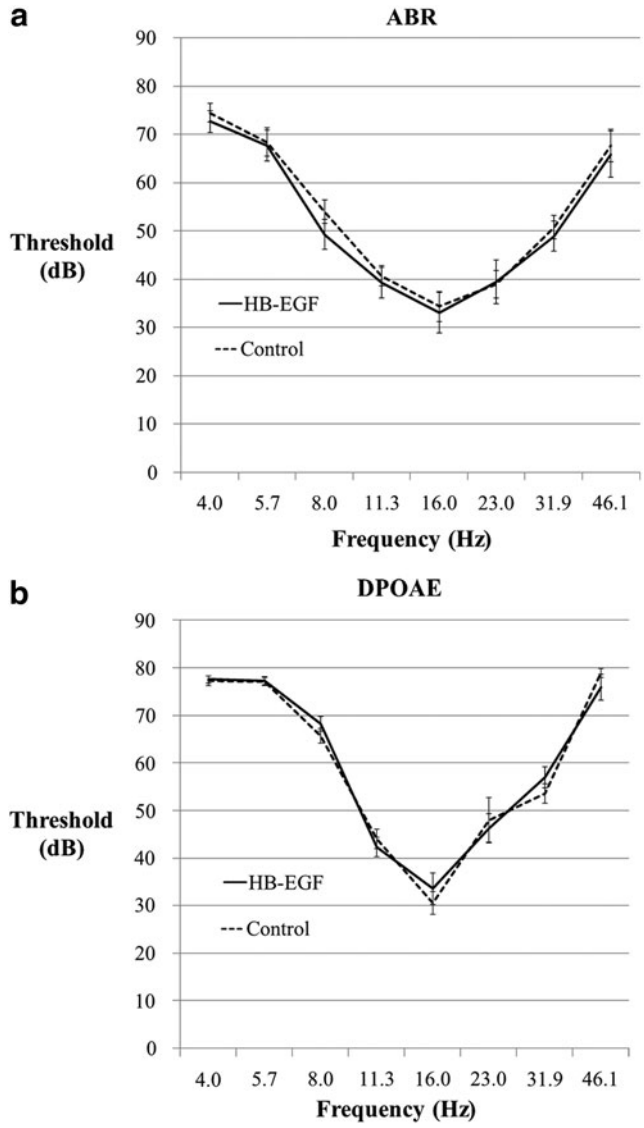

FIG. 6. The auditory brainstem response (ABR) and distortion product otoacoustic emission (DPOAE) thresholds of HB-EGF-treated ears compared with control. Figure shows the **(a)** ABR and **(b)** DPOAE thresholds measured at 10 weeks in ears perforated and injected with the polymer hydrogel loaded with HB-EGF at 50 μg/mL ($n = 13$), 10 times the effective dose, compared with control ears, which were injected with the polymer hydrogel only ($n = 13$). There were no differences between groups demonstrating a lack of ototoxicity of HB-EGF in the mouse model.

is needed for the closure of TM wounds, KB-R7785 was used to inhibit TM wound healing in mice and create a chronic perforation (lasting 3 months). Our results show that keratinocyte migration induced by EGFR ligand shedding is needed for normal healing of the TM and is likely to be a mechanism for the development of chronic TM perforations. KB-R7785 inhibition of TM wound healing provides a reliable, reproducible, and universally available chronic TM perforation animal model providing a platform for which to test other treatments for TM wound healing.[33]

TM perforations in the clinical setting are known to heal differently depending on their environment.[34] One of the main factors affecting healing is ET dysfunction.[7] ET dysfunction may lead to the infection or inflammation, which, then in turn, we hypothesize, inhibits keratinocyte migration through inhibition of EGFR ligand shedding. To better mimic the human condition, we then created a second mouse model of chronic TM perforation in the setting of ET dysfunction. This is the first published model of chronic perforation in the setting of ET dysfunction. This model can be reliably reproduced with practice of the surgical technique described in the methods.

The ability to design better interventions for TM perforations has been limited by the lack of suitable chronic TM perforation animal models. Research in this field has been relied on testing on acute perforations. But, in current models, all laboratory created perforations heal spontaneously. This devalues the intervention and makes the efficacy in chronic TM perforations debatable.[24,33] All current animal models for chronic TM perforation are not suitable because they are either too destructive and prevent their use in further wound healing treatment studies, create wounds not comparable to real life or are too difficult to be replicated in subsequent studies.[33] To address this deficiency we aimed to develop animal models that closely mimic the human condition. Until now, there has been no animal model for CSOM.

A suitable CSOM model is one that mimics the human condition. To do this it requires three components: a chronic perforation, ET dysfunction, and bacterial suppuration.[35] Without a chronic perforation, the model is only an acute suppurative otitis media model. In particular, it is important to induce ET dysfunction with bacteria to mimic human CSOM as ET occlusion can induce pathogenic behavior of normal bacteria in the middle ear.[36] In acknowledgement of the desired characteristics of an animal model of CSOM, we adopted our mice model with chronic perforations following ET occlusion surgery and KB-R7785 application and inoculated them with *Pseudomonas aeruginosa*. The uniqueness of pseudomonas to form a chronic infection in this setting is reflected in the human setting with it being the most common isolate in human CSOM.[35] The mucoepithelial junction in chronic TM perforations can be found in different locations[37] with the connective tissue containing inflammatory cells and in some cases demonstrates extensive fibrosis, bone-like deposits, and irregular, poorly arranged fibroblasts.[38] In our CSOM model, the perforation edge shows a mucosal layer migrated laterally to be directly adjacent to the keratinocyte layer with a thickened fibrous layer containing inflammatory cells. These findings add further validation to this model.

The mouse provides an ideal model for middle ear research. Rats and mice both are the best nonprimate model for TM research.[33] The benefits associated with the use of mice include availability, low financial cost, a similar TM structure to humans,[39,40] and an easily accessible TM through their external ear canal. The mouse ET is similar to the human child ET.[41] In planning for our ET occlusion model, practice procedures were formed, the mice sacrificed, and the ETs were examined postmortem to confirm that the technique provided complete occlusion of the ET. The bacteria and concentrations used in our models were chosen based on previous success in the literature in animal models of acute otitis media[25,42–82] Our chosen concentrations represented concentrations previously shown to create otitis media

without animal mortality. The 2 week period for testing after inoculation was chosen based on the clinical studies of CSOM that report bacterial exudate persisting for 2 weeks in a chronic perforation is what defines human CSOM.[4]

HB-EGF is from the EGF family of growth factors. EGF family members can induce juxtacrine, autocrine, paracrine, or endocrine signaling depending on the cellular environment because they are cleaved from the membrane by metalloproteinases to form the mature soluble growth factor.[83] Members of the EGF family have differing binding activity to the EGFR family. There are four identified members of the EGFR family (HER1, HER2, HER3, and HER4). They are structurally related tyrosine kinases with a single membrane spanning domain and a domain within the cytoplasm.[84,85] Unlike EGF, HB-EGF binds to both HER1 and HER4.[86–88] Betacellulin and Neuregulin2 also bind to HER1 and HER4.[89–91] Pro HB-EGF is synthesized as a type I single transmembrane precursor protein that then undergoes extensive proteolytic processing termed ectodomain shedding.[92–95] This releases the soluble mature form of HB-EGF. HB-EGF contains an EGF-like domain thought to be required for EGF family members to bond and activate EGFR.[96] HB-EGF decreases epithelial markers such as keratins 1, 5, 10, and 14 while increasing cell motility genes such as SNA1, ZEB1, COX-2, and MMP1[97] The metalloproteinases (including ADAM 9, 10, 12, 17) responsible for ectodomain shedding of pro HB-EGF predominantly regulate the binding of mature HB-EGF and regulate activation of EGFRs.[93,98–101]

HB-EGF then acts through both EGFR-dependent and EGFR-independent mechanisms. Our results show that HB-EGF can induce keratinocyte migration in a chronic TM perforation to close the perforation and create a histologically comparable healed TM. For HB-EGF to be applicable in the clinical setting it is important to demonstrate nonototoxicity. Before human clinical trials, nonototoxicity should also be demonstrated in a second nonrodent animal model, but these initial results are promising. These results provide the groundwork for further preclinical studies in translation toward human clinical studies, including more work to be done to demonstrate safety. Significant systemic absorption from topical delivery should also be excluded. Based on single, local administration of HB-EGF, no systemic exposure is expected in humans. Additionally, there is literature available on toxicity and toxicokinetics of HB-EGF after IV and intrabladder dosing for up to 28 days in female SD rats. No toxicity attributable to HB-EGF was observed in the study at doses of up to 30 μg/kg for 28 days.[102]

To treat chronic TM perforations, an ideal approach would be to have a liquid that can be dropped into the ear, which then hardens and slowly resorbs over a designated time frame while releasing a bioactive substance at a steady concentration. This type of sustained release topical eardrop is not commercially available. Based on our previous work to deliver bioactive substances in bone, we further developed a biocompatible, bioresorbable, injectable polymer for use in the ear.[21,22,103] Our hydrogel consists of two main polymers, which are hydrophilic chitosan backbone molecules and hydrophobic polylactide side chains, together with fibrinogen molecules. All three compounds are nontoxic and biodegradable.[104–106] The fibrinogen incorporation improves growth factor binding affinity, enhances cell attachment, and provides proteolytically degradable sites. Drug release from the polymeric hydrogel varies according to the characteristics such as hydrophilic affinity, swelling behavior, degradability, and crosslinking density of the polymer. The heparin binding domains of fibrinogen within the polymer also have additional wound healing benefits. Sodium metabisulfite is used as the catalyst for crosslinking and has the additional benefit of antibacterial properties useful in inhibiting the growth of bacteria in CSOM. Our results demonstrate that the hydrogel used is nonototoxic in the mouse model.

In summary, HB-EGF delivered by a biodegradable injectable hydrogel polymer is promising as a treatment for chronic TM perforation and CSOM. This treatment could address the large worldwide unmet need for a nonsurgical way to repair TM perforations.

Acknowledgments

The authors thank Dr. Shigeki's laboratory, Ehime University Japan, for supplying initial OSU8-1 for use in our animal models, support from the Garnett Passe and Rodney Williams Memorial Foundation, support from Stanford's SPARK, support from the Stanford Child Health Research Institute, support from NIH R01AR057837 (NIAMS, Y.P.Y.), NIH R01DE021468 (NIDCR, Y.P.Y.), DOD W81XWH-10-1-0966 (PRORP, Y.P.Y.), and Wallace H. Coulter Foundation (Y.P.Y.).

Disclosure Statement

Filed patents: U.S. Non Provisional No. 61/823,749, April 2014 (P.S.M., S.K., Y.P.Y.) and U.S. Non Provisional No. 61/810,101, April 2014 (S.K., Y.P.Y.)

References

1. Acuin, J. Chronic Suppurative Otitis Media: Burden of Illness and Management Options. Switzerland: World Health Organisation, 2004.
2. Karela, M., Berry, S., Watkins, A., and Phillipps, JJ. Myringoplasty: surgical outcomes and hearing improvement: is it worth performing to improve hearing? Eur Arch Otorhinolaryngol **265,** 1039, 2008.
3. Aggarwal, R., Saeed, S.R., and Green, K.J. Myringoplasty. J Laryngol Otol **120,** 429, 2006.
4. Monasta, L., Ronfani, L., Marchetti, F., Montico, M., Vecchi Brumatti, L., Bavcar, A., *et al.* Burden of disease caused by otitis media: systematic review and global estimates. PLoS One **7,** e36226, 2012.
5. Jackler, R.K. A regenerative method of tympanic membrane repair could be the greatest advance in otology since the cochlear implant. Otol Neurotol **33,** 289, 2012.
6. Santa Maria, P.L., and Oghalai, J.S. Is office-based myringoplasty a suitable alternative to surgical tympanoplasty? Laryngoscope **124,** 1053, 2014.
7. Gladstone, H.B., Jackler, R.K., and Varav, K. Tympanic membrane wound healing. An overview. Otolaryngol Clin North Am **28,** 913, 1995.
8. Hong, P., Bance, M., and Gratzer, P.F. Repair of tympanic membrane perforation using novel adjuvant therapies: a contemporary review of experimental and tissue engineering studies. Int J Pediatr Otorhinolaryngol **77,** 3, 2013.
9. Kaftan, H., Reuther, L., Miehe, B., Hosemann, W., and Beule, A. Inhibition of fibroblast growth factor receptor 1:

influence on tympanic membrane wound healing in rats. Eur Arch Otorhinolaryngol **269,** 87, 2012.
10. Kato, M., and Jackler, R.K. Repair of chronic tympanic membrane perforations with fibroblast growth factor. Otolaryngol Head Neck Surg **115,** 538, 1996.
11. Hakuba, N., Taniguchi, M., Shimizu, Y., Sugimoto, A., Shinomori, Y., and Gyo, K. A new method for closing tympanic membrane perforations using basic fibroblast growth factor. Laryngoscope **113,** 1352, 2003.
12. Hakuba, N., Iwanaga, M., Tanaka, S., Hiratsuka, Y., Kumabe, Y., Konishi, M., *et al.* Basic fibroblast growth factor combined with atelocollagen for closing chronic tympanic membrane perforations in 87 patients. Otol Neurotol **31,** 118, 2010.
13. Kanemaru, S., Umeda, H., Kitani, Y., Nakamura, T., Hirano, S., and Ito, J. Regenerative treatment for tympanic membrane perforation. Otol Neurotol **32,** 1218, 2011.
14. Yeo, S.W., Kim, S.W., Suh, B.D., and Cho, S.H. Effects of platelet-derived growth factor-AA on the healing process of tympanic membrane perforation. Am J Otolaryngol **21,** 153, 2000.
15. Roosli, C., von Buren, T., Gassmann, N.B., and Huber, A.M. The impact of platelet-derived growth factor on closure of chronic tympanic membrane perforations: a randomized, double-blind, placebo-controlled study. Otol Neurotol **32,** 1224, 2011.
16. Chauvin, K., Bratton, C., and Parkins, C. Healing large tympanic membrane perforations using hyaluronic acid, basic fibroblast growth factor, and epidermal growth factor. Otolaryngol Head Neck Surg **121,** 43, 1999.
17. Hellstrom, S., and Laurent, C. Hyaluronan and healing of tympanic membrane perforations. An experimental study. Acta Otolaryngol Suppl **442,** 54, 1987.
18. Laurent, C., Hellstrom, S., and Fellenius, E. Hyaluronan improves the healing of experimental tympanic membrane perforations. A comparison of preparations with different rheologic properties. Arch Otolaryngol Head Neck Surg **114,** 1435, 1988.
19. Kaftan, H., Reuther, L., Miehe, B., Hosemann, W., and Herzog, M. Delay of tympanic membrane wound healing in rats with topical application of a tyrosine kinase inhibitor. Wound Repair Regen **16,** 364, 2008.
20. Ramsay, H.A., Heikkonen, E.J., and Laurila, P.K. Effect of epidermal growth factor on tympanic membranes with chronic perforations: a clinical trial. Otolaryngol Head Neck Surg **113,** 375, 1995.
21. Kim, S., Kang, Y., Krueger, C.A., Sen, M., Holcomb, J.B., Chen, D., *et al.* Sequential delivery of BMP-2 and IGF-1 using a chitosan gel with gelatin microspheres enhances early osteoblastic differentiation. Acta Biomater **8,** 1768, 2012.
22. Kim, S., Tsao, H., Kang, Y., Young, D.A., Sen, M., and Wenke, J.C., *et al. In vitro* evaluation of an injectable chitosan gel for sustained local delivery of BMP-2 for osteoblastic differentiation. J Biomed Mater Res B Appl Biomater **99,** 380, 2011.
23. Santa Maria, P.L. In response to: regeneration of chronic tympanic membrane perforation using an EGF-releasing chitosan patch. Tissue Eng Part A **19,** 2109, 2013.
24. Santa Maria, P.L., Redmond, S.L., Atlas, M.D., and Ghassemifar, R. Histology of the healing tympanic membrane following perforation in rats. Laryngoscope **120,** 2061, 2010.
25. Hebda, P.A., Piltcher, O.B., Swarts, J.D., Alper, C.M., Zeevi, A., and Doyle, W.J. Cytokine profiles in a rat model of otitis media with effusion caused by Eustachian tube obstruction with and without *Streptococcus pneumoniae* infection. Laryngoscope **112,** 1657, 2002.
26. Tokumaru, S., Higashiyama, S., Endo, T., Nakagawa, T., Miyagawa, J.I., Yamamori, K., *et al.* Ectodomain shedding of epidermal growth factor receptor ligands is required for keratinocyte migration in cutaneous wound healing. J Cell Biol **151,** 209, 2000.
27. Xia, A., Visosky, A.M., Cho, J.H., Tsai, M.J., Pereira, F.A., and Oghalai, J.S. Altered traveling wave propagation and reduced endocochlear potential associated with cochlear dysplasia in the BETA2/NeuroD1 null mouse. J Assoc Res Otolaryngol **8,** 447, 2007.
28. Shirakata, Y., Kimura, R., Nanba, D., Iwamoto, R., Tokumaru, S., Morimoto, C., *et al.* Heparin-binding EGF-like growth factor accelerates keratinocyte migration and skin wound healing. J Cell Sci **118,** 2363, 2005.
29. El-Seifi, A., and Fouad, B. Granular myringitis: is it a surgical problem? Am J Otol **21,** 462, 2000.
30. Fagan, P., and Patel, N. A hole in the drum. An overview of tympanic membrane perforations. Aust Fam Physician **31,** 707, 2002.
31. Lazarus, G.S., Cooper, D.M., Knighton, D.R., Percoraro, R.E., Rodeheaver, G., and Robson, M.C. Definitions and guidelines for assessment of wounds and evaluation of healing. Wound Repair Regen **2,** 165, 1994.
32. Santa Maria, P.L., Redmond, S.L., McInnes, R.L., Atlas, M.D., and Ghassemifar, R. Tympanic membrane wound healing in rats assessed by transcriptome profiling. Laryngoscope **121,** 2199, 2011.
33. Santa Maria, P.L., Atlas, M.D., and Ghassemifar, R. Chronic tympanic membrane perforation: a better animal model is needed. Wound Repair Regen **15,** 450, 2007.
34. Wielinga, E.W., Peters, T.A., Tonnaer, E.L., Kuijpers, W., and Curfs, J.H. Middle ear effusions and structure of the tympanic membrane. Laryngoscope **111,** 90, 2001.
35. Verhoeff, M., van der Veen, E.L., Rovers, M.M., Sanders, E.A., and Schilder, A.G. Chronic suppurative otitis media: a review. Int J Pediatr Otorhinolaryngol **70,** 1, 2006.
36. Kuijpers, W., and van der Beek, J.M. The role of microorganisms in experimental Eustachian tube obstruction. Acta Otolaryngol Suppl **414,** 58, 1984.
37. Somers, T., Houben, V., Goovaerts, G., Govaerts, P.J., and Offeciers, F.E. Histology of the perforated tympanic membrane and its muco-epithelial junction. Clin Otolaryngol **22,** 162, 1997.
38. Spandow, O., Hellstrom, S., and Dahlstrom, M. Structural characterization of persistent tympanic membrane perforations in man. Laryngoscope **106,** 346, 1996.
39. Schmidt, S.H., and Hellstrom, S. Tympanic-membrane structure—new views. A comparative study. ORL J Otorhinolaryngol Relat Spec **53,** 32, 1991.
40. Chole, R.A., and Kodama, K. Comparative histology of the tympanic membrane and its relationship to cholesteatoma. Ann Otol Rhinol Laryngol **98,** 761, 1989.
41. Albiin, N. The anatomy of the Eustachian tube. Acta Otolaryngol Suppl **414,** 34, 1984.
42. Trinidad, A., Ramirez-Camacho, R., Garcia-Berrocal, J.R., Verdaguer, J.M., Vicente, J., and Daza, R. Tissular changes induced by *Pseudomonas aeruginosa* in an otitis media rat model with tubal obstruction. Acta Otolaryngol **127,** 132, 2007.
43. Trinidad, A., Ramirez-Camacho, R., Garcia-Berrocal, J.R., Verdaguer, J.M., Vicente, J., and Pinilla, M.T. *Pseudomonas*

aeruginosa infection in the hypoventilated middle ear: an experimental model. Acta Otolaryngol **125,** 266, 2005.
44. Lewis, D.M., Schram, J.L., Meadema, S.J., and Lim, D.J. Experimental otitis media in chinchillas. Ann Otol Rhinol Laryngol Suppl **89,** 344, 1980.
45. Watanabe, N., Briggs, B.R., and Lim, D.J. Experimental otitis media in chinchillas. I. Baseline immunological investigation. Ann Otol Rhinol Laryngol Suppl **93,** 1, 1982.
46. Sato, K., Liebeler, C.L., Quartey, M.K., Le, C.T., and Giebink, G.S. Middle ear fluid cytokine and inflammatory cell kinetics in the chinchilla otitis media model. Infect Immun **67,** 1943, 1999.
47. Hoa, M., Syamal, M., Sachdeva, L., Berk, R., and Coticchia, J. Demonstration of nasopharyngeal and middle ear mucosal biofilms in an animal model of acute otitis media. Ann Otol Rhinol Laryngol **118,** 292, 2009.
48. Giebink, G.S., Payne, E.E., Mills, E.L., Juhn, S.K., and Quie, P.G. Experimental otitis media due to *Streptococcus pneumoniae*: immunopathogenic response in the chinchilla. J Infect Dis **134,** 595, 1976.
49. Watanabe, N., DeMaria, T.F., Lewis, D.M., Mogi, G., and Lim, D.J. Experimental otitis media in chinchillas. II. Comparison of the middle ear immune responses to S pneumoniae types 3 and 23. Ann Otol Rhinol Laryngol Suppl **93,** 9, 1982.
50. Stol, K., van Selm, S., van den Berg, S., Bootsma, H.J., Blokx, W.A., Graamans, K., *et al.* Development of a non-invasive murine infection model for acute otitis media. Microbiology **155,** 4135, 2009.
51. Sautter, N.B., Delaney, K.L., Hausman, F.A., and Trune, D.R. Tissue remodeling in the acute otitis media mouse model. Int J Pediatr Otorhinolaryngol **75,** 1368, 2011.
52. Sabharwal, V., Figueira, M., Pelton, S.I., and Pettigrew, M.M. Virulence of *Streptococcus pneumoniae* serotype 6C in experimental otitis media. Microbes Infect **14,** 712, 2012.
53. Giebink, G.S., and Quie, P.G. Comparison otitis media due to types 3 and 23 *Streptococcus pneumoniae* in the Chinchilla model. J Infect Dis **136,** S191, 1977.
54. Giebink, G.S., Berzins, I.K., Marker, S.C., and Schiffman, G. Experimental otitis media after nasal inoculation of *Streptococcus pneumoniae* and influenza A virus in chinchillas. Infect Immun **30,** 445, 1980.
55. Larsson, C., Dirckx, J.J., Decraemer, W.F., Bagger-Sjoback, D., and von Unge, M. Pars flaccida displacement pattern in purulent otitis media in the gerbil. Otol Neurotol **24,** 358, 2003.
56. von Unge, M., Decraemer, W.F., Bagger-Sjoback, D., and Van den Berghe, D. Tympanic membrane changes in experimental purulent otitis media. Hear Res **106,** 123, 1997.
57. Parks, R.R., Huang, C.C., and Haddad, J., Jr. Middle ear catalase distribution in an animal model of otitis media. Eur Arch Otorhinolaryngol **253,** 445, 1996.
58. Melhus, A., and Ryan, A.F. A mouse model for acute otitis media. APMIS **111,** 989, 2003.
59. MacArthur, C.J., Hefeneider, S.H., Kempton, J.B., Parrish, S.K., McCoy, S.L., and Trune, D.R. Evaluation of the mouse model for acute otitis media. Hear Res **219,** 12, 2006.
60. Lv, Y.X., Zhao, S.P., Zhang, J.Y., Zhang, H., Xie, Z.H., Cai, G.M., *et al.* Effect of orange peel essential oil on oxidative stress in AOM animals. Int J Biol Macromol **50,** 1144, 2012.
61. Forseni Flodin, M. Macrophages and possible osteoclast differentiation in the rat bullar bone during experimental acute otitis media, with reference to tympanosclerosis. Otol Neurotol **22,** 771, 2001.
62. Yoon, Y.J., and Hellstrom, S. Ultrastructural characteristics of the round window membrane during pneumococcal otitis media in rat. J Korean Med Sci **17,** 230, 2002.
63. Hodges, K.B., Penny, J.E., Brown, R.D., and Henley, C.M. Scanning electron microscopy of the cochlea in rats with *Streptococcus pneumoniae* otitis media. Arch Otolaryngol **110,** 429, 1984.
64. Eriksson, P.O., Mattsson, C., and Hellstrom, S. First forty-eight hours of developing otitis media: an experimental study. Ann Otol Rhinol Laryngol **112,** 558, 2003.
65. Eriksson, P.O., and Hellstrom, S. Acute otitis media develops in the rat after intranasal challenge of *Streptococcus pneumoniae*. Laryngoscope **113,** 2047, 2003.
66. Raustyte, G., and Hermansson, A. Development of myringosclerosis during acute otitis media caused by *Streptococcus pneumoniae* and non-typeable Haemophilus influenzae: a clinical otomicroscopical study using the rat model. Medicina **41,** 661, 2005.
67. Spratley, J., Hellstrom, S., Eriksson, P.O., and Pais-Clemente, M. Myringotomy delays the tympanic membrane recovery in acute otitis media: a study in the rat model. Laryngoscope **112,** 1474, 2002.
68. Hermansson, A., Emgard, P., Prellner, K., and Hellstrom, S. A rat model for bacterial otitis media. Acta Otolaryngol Suppl **457,** 144, 1989.
69. Magnuson, K., and Hellstrom, S. Early structural changes in the rat tympanic membrane during pneumococcal otitis media. Eur Arch Otorhinolaryngol **251,** 393, 1994.
70. Tonnaer, E.L., Sanders, E.A., and Curfs, J.H. Bacterial otitis media: a new non-invasive rat model. Vaccine **21,** 4539, 2003.
71. van der Ven, L.T., van den Dobbelsteen, G.P., Nagarajah, B., van Dijken, H., Dortant, P.M., Vos, J.G., *et al.* A new rat model of otitis media caused by *Streptococcus pneumoniae*: conditions and application in immunization protocols. Infect Immun **67,** 6098, 1999.
72. Fogle-Ansson, M., White, P., Hermansson, A., and Melhus, A. Otomicroscopic findings and systemic interleukin-6 levels in relation to etiologic agent during experimental acute otitis media. APMIS **114,** 285, 2006.
73. Hermansson, A., Emgard, P., Prellner, K., and Hellstrom, S. A rat model for pneumococcal otitis media. Am J Otolaryngol **9,** 97, 1988.
74. Melhus, A., and Ryan, A.F. Expression of cytokine genes during pneumococcal and nontypeable Haemophilus influenzae acute otitis media in the rat. Infect Immun **68,** 4024, 2000.
75. Melhus, A., and Ryan, A.F. Expression of molecular markers for bone formation increases during experimental acute otitis media. Microb Pathog **30,** 111, 2001.
76. Li-Korotky, H.S., Swarts, J.D., Hebda, P.A., and Doyle, W.J. Cathepsin gene expression profile in rat acute pneumococcal otitis media. Laryngoscope **114,** 1032, 2004.
77. Hebda, P.A., Alper, C.M., Doyle, W.J., Burckart, G.J., Diven, W.F., and Zeevi, A. Upregulation of messenger RNA for inflammatory cytokines in middle ear mucosa in a rat model of acute otitis media. Ann Otol Rhinol Laryngol **107,** 501, 1998.
78. Tsuboi, Y., Kim, Y., Paparella, M.M., Chen, N., Schachern, P.A., and Lin, J. Pattern changes of mucin gene expression with pneumococcal otitis media. Int J Pediatr Otorhinolaryngol **61,** 23, 2001.

79. Chen, A., Li, H.S., Hebda, P.A., Zeevi, A., and Swarts, J.D. Gene expression profiles of early pneumococcal otitis media in the rat. Int J Pediatr Otorhinolaryngol **69,** 1383, 2005.
80. Aladag, I., Guven, M., Eyibilen, A., Sahin, S., and Koseoglu, D. Efficacy of vitamin A in experimentally induced acute otitis media. Int J Pediatr Otorhinolaryngol **71,** 623, 2007.
81. Piltcher, O.B., Swarts, J.D., Magnuson, K., Alper, C.M., Doyle, W.J., and Hebda, P.A. A rat model of otitis media with effusion caused by Eustachian tube obstruction with and without *Streptococcus pneumoniae* infection: methods and disease course. Otolaryngol Head Neck Surg **126,** 490, 2002.
82. Li, J.D., Hermansson, A., Ryan, A.F., Bakaletz, L.O., Brown, S.D., Cheeseman, M.T., *et al.* Panel 4: recent advances in otitis media in molecular biology, biochemistry, genetics, and animal models. Otolaryngol Head Neck Surg **148,** E52, 2013.
83. Singh, A.B., and Harris, R.C. Autocrine, paracrine and juxtacrine signaling by EGFR ligands. Cell Signal **17,** 1183, 2005.
84. Plowman, G.D., Culouscou, J.M., Whitney, G.S., Green, J.M., Carlton, G.W., Foy, L., *et al.* Ligand-specific activation of HER4/p180erbB4, a fourth member of the epidermal growth factor receptor family. Proc Natl Acad Sci U S A **90,** 1746, 1993.
85. Taylor, S.R., Markesbery, M.G., and Harding, P.A. Heparin-binding epidermal growth factor-like growth factor (HB-EGF) and proteolytic processing by a disintegrin and metalloproteinases (ADAM): a regulator of several pathways. Semin Cell Dev Biol **28,** 22, 2014.
86. Higashiyama, S., Lau, K., Besner,G.E, Abraham, J.A., and Klagsbrun, M. Structure of heparin-binding EGF-like growth factor. Multiple forms, primary structure, and glycosylation of the mature protein. J Biol Chem **267,** 6205, 1992.
87. Elenius. K., Paul, S., Allison, G., Sun, J., Klagsbrun, M. Activation of HER4 by heparin-binding EGF-like growth factor stimulates chemotaxis but not proliferation. EMBO J **16,** 1268, 1997.
88. Higashiyama, S., Abraham, J.A., Miller, J., Fiddes, J.C., and Klagsbrun, M. A heparin-binding growth factor secreted by macrophage-like cells that is related to EGF. Science **251,** 936, 1991.
89. Chang, H., Riese, D.J., 2nd., Gilbert, W., Stern, D.F., McMahan, U.J. Ligands for ErbB-family receptors encoded by a neuregulin-like gene. Nature **387,** 509, 1997.
90. Carraway, K.L., 3rd., Weber, J.L., Unger, M.J., Ledesma, J., Yu, N., Gassmann, M., *et al.* Neuregulin-2, a new ligand of ErbB3/ErbB4-receptor tyrosine kinases. Nature **387,** 512, 1997.
91. Shing, Y., Christofori, G., Hanahan, D., Ono, Y., Sasada, R., Igarashi, K., *et al.* Betacellulin: a mitogen from pancreatic beta cell tumors. Science **259,** 1604, 1993.
92. Yan, Y., Shirakabe, K., and Werb, Z. The metalloprotease Kuzbanian (ADAM10) mediates the transactivation of EGF receptor by G protein-coupled receptors. J Cell Biol **158,** 221, 2002.
93. Asakura, M., Kitakaze, M., Takashima, S., Liao, Y., Ishikura, F., Yoshinaka, T., *et al.* Cardiac hypertrophy is inhibited by antagonism of ADAM12 processing of HB-EGF: metalloproteinase inhibitors as a new therapy. Nat Med **8,** 35, 2002.
94. Izumi, Y., Hirata, M., Hasuwa, H., Iwamoto, R., Umata, T., Miyado, K., *et al.* A metalloprotease-disintegrin, MDC9/meltrin-gamma/ADAM9 and PKCdelta are involved in TPA-induced ectodomain shedding of membrane-anchored heparin-binding EGF-like growth factor. EMBO J **17,** 7260, 1998.
95. Nakagawa, T., Higashiyama, S., Mitamura, T., Mekada, E., and Taniguchi, N. Amino-terminal processing of cell surface heparin-binding epidermal growth factor-like growth factor up-regulates its juxtacrine but not its paracrine growth factor activity. J Biol Chem **271,** 30858, 1996.
96. Thompson, S.A., Higashiyama, S., Wood, K., Pollitt, N.S., Damm, D., McEnroe, G., *et al.* Characterization of sequences within heparin-binding EGF-like growth factor that mediate interaction with heparin. J Biol Chem **269,** 2541, 1994.
97. Stoll, S.W., Rittie, L., Johnson, J.L., and Elder, J.T. Heparin-binding EGF-like growth factor promotes epithelial-mesenchymal transition in human keratinocytes. J Invest Dermatol **132,** 2148, 2012.
98. Cisse, M.A., Sunyach, C., Lefranc-Jullien, S., Postina, R., Vincent, B., and Checler, F. The disintegrin ADAM9 indirectly contributes to the physiological processing of cellular prion by modulating ADAM10 activity. J Biol Chem **280,** 40624, 2005.
99. Peschon, J.J., Slack, J.L., Reddy, P., Stocking, K.L., Sunnarborg, S.W., Lee, D.C., *et al.* An essential role for ectodomain shedding in mammalian development. Science **282,** 1281, 1998.
100. Sahin, U., Blobel, C.P. Ectodomain shedding of the EGF-receptor ligand epigen is mediated by ADAM17. FEBS Lett **581,** 41, 2007.
101. Sahin, U., Weskamp, G., Kelly, K., Zhou, H.M., Higashiyama, S., Peschon, J., *et al.* Distinct roles for ADAM10 and ADAM17 in ectodomain shedding of six EGFR ligands. J Cell Biol **164,** 769, 2004.
102. Coowanitwong, I., Keay, S.K., Natarajan, K., Garimella, T.S., Mason, C.W., Grkovic, D., *et al.* Toxicokinetic study of recombinant human heparin-binding epidermal growth factor-like growth factor (rhHB-EGF) in female Sprague Dawley rats. Pharm Res **25,** 542, 2008.
103. Kim, S., Kang, Y., Mercado-Pagan, A.E., Maloney, W.J., and Yang, Y. *In vitro* evaluation of photo-crosslinkable chitosan-lactide hydrogels for bone tissue engineering. J Biomed Mater Res B Appl Biomater **102,** 1393, 2014.
104. Bhattarai, N., Ramay, H.R., Chou, S.H., and Zhang, M. Chitosan and lactic acid-grafted chitosan nanoparticles as carriers for prolonged drug delivery. Int J Nanomed **1,** 181, 2006.
105. Liu, Y., Tian, F., and Hu, K.A. Synthesis and characterization of a brush-like copolymer of polylactide grafted onto chitosan. Carbohydr Res **339,** 845, 2004.
106. Janmey, P.A., Winer, J.P., and Weisel, J.W. Fibrin gels and their clinical and bioengineering applications. J R Soc Interface **6,** 1, 2009.

Address correspondence to:
Peter Luke Santa Maria, MBBS, PhD
Department of Otolaryngology, Head and Neck Surgery
Stanford University
801 Welch Road
Stanford, CA 94035

E-mail: psantamaria@ohns.stanford.edu

Received: August 6, 2014
Accepted: January 7, 2015
Online Publication Date: March 13, 2015